Available online at www.sciencedirect.com
SCIENCE DIRECT®
Journal of Photochemistry and Photobiology A: Chemistry 171 (2005) 231–236
Journal of Photochemistry and Photobiology A:Chemistry
www.elsevier.com/locate/jphotochem

Novel cyanine dyes with different methine chains as sensitizers for nanocrystalline solar cell

Xiuying Chen[a], Jiahao Guo[b,c], Xiaojun Peng[a,*], Min Guo[b], Yongqian Xu[a], Lei Shi[a], Chunli Liang[a], Li Wang[a], Yunling Gao[a], Shiguo Sun[a], Shengmin Cai[b,**]

[a] *State key laboratory of fine chemicals, Dalian University of Technology, Dalian 116012, PR China*
[b] *College of Chemistry and Molecular Engineering, Peking University, Beijing 100871, PR China*
[c] *Department of Chemistry, China West Normal University, Sichuan Nanchong 637002, PR China*

Received 21 July 2004; received in revised form 14 October 2004; accepted 22 October 2004
Available online 8 December 2004

Abstract

Novel cyanine dyes (Sqb and Cyb3) with carboxylbenzyl group and different methine chains as solar cell sensitizers were synthesized and the photoelectrochemical behaviors of the TiO_2 nanocrystalline electrode sensitized by them were investigated. The results show that I_{sc} (2.76 mA/cm^2), monochromatic incident photon-to-current conversion efficiency (IPCE) (46%) and η (1.7%) of TiO_2 nanocrystalline solar cell sensitized by Sqb were higher than that of TiO_2 nanocrystalline solar cell sensitized by Cyb3 when TiO_2 nanostructured porous film was 6.5 μm thick and was sensitized for 6 h and 4 h, respectively. The excited state level of these dyes matches the conductive band edge of TiO_2 nanoparticles. Therefore, the sensitization of the dyes can increase the photocurrent density of TiO_2 nanocrystalline electrode.

Keywords: TiO_2 nanocrystalline electrode; Photoelectric conversion; Dye-sensitized solar cell; Squarylium dye; Cyanine dye

1. Introduction

Increasing attention [1,2] has been focused on nanocrystalline TiO_2 electrode sensitized by organic photosensitized dye since Grätzel [3] utilized *cis*-Ru[4,4′-(LL)]$_2$(NCS)$_2$, (L = 2,2′-bipyridyl-4,4′-dicarboxylate) to sensitized TiO_2 nanocrystalline and photoelectric transfer efficiency can be up to 10%. Compared to the ruthenium bipyridyl complex, organic dyes are easier to be synthesized and cost less. Recently, organic dye-sensitized TiO_2 solar cells have made great progress, and the highest overall yield of solar cells sensitized by organic dyes has exceeded 6% [4,5]. To obtain high efficient photosensitizer for solar cells material, the investigation on new dyes with improved molecular structure is necessary. Cyanine dyes have intense and broad absorption band in the visible and near-infrared regions, and excellent sensitizing properties in photography. However, few works have been done on their application as sensitizers for solar cells. Sayama studied merocyanines with different chain length (–(CH$_2$)$_n$–COOH) anchoring on TiO_2 surface via ester group and found that IPCE value of the TiO_2 electrode sensitized by various dyes increased with the decrease of the distance from dye chromophore to TiO_2 surface, which is very worthwhile to design a new sensitizer [6]. Simultaneously, they found that the increase of methine chain (–(CH=CH)$_m$–) of the dyes enhances the difficulty of the electron transfer from the excited dye to the conduction band of TiO_2 [7]. As organic sensitizers for nanocrystalline solar cell material, the high photostabilities of the dyes play a significant role in photoelectrochemical applications. Chen synthesized *N*-benzylindotricarbocyanine dyes and found that introduction of large benzyl group on nitrogen atom improved the photostability greatly [8]. In this article, we report the synthesis and photoelectric properties of novel cyanine dye (Cyb3) and squarylium dye (Sqb) with

* Corresponding author. Tel.: +86 411 8899 3899; fax: +86 411 8899 3885.
** Co-corresponding author. Tel. +86 10 62751728.
E-mail addresses: pengxj@dlut.edu.cn (X. Peng), caism@pku.edu.cn (S. Cai).

1010-6030/$ – see front matter © 2004 Elsevier B.V. All rights reserved.
doi:10.1016/j.jphotochem.2004.10.016

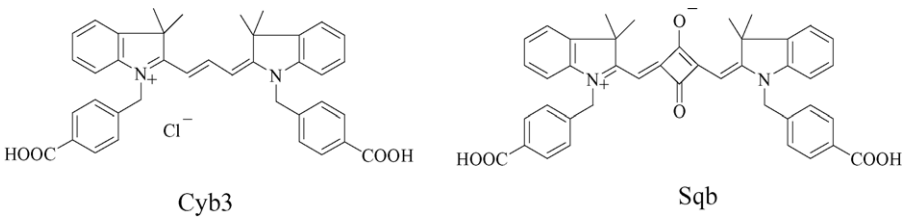

Fig. 1. Structures of Cyb3 and Sqb.

common 3*H*-indole-*N*-carboxylbenzyl groups anchoring on nano-TiO_2 and two different kinds of methine chains (Fig. 1).

2. Experiments

2.1. Materials and instruments

Oxide of indium and stannum were used as the photoanode electric fundus (South Glass Science and Technology Holding Ltd., China). All other chemicals and solvents involved were analytical reagents of the highest available purity. Redistilled water was used for the solution. ^{1}H NMR spectra were recorded on a Varian INOVA 400M NMR spectrometer and elemental analysis were performed on a PE 2400 II elemental analyzer.

2.2. Synthesis

2,3,3-Trimethyl-3*H*-indolenine (1) was synthesized according to ref [9].

N-(4-Carboxyl)benzyl-3,3-dimethyl-3*H*-indolenine quaternary salt (2): 1.59 g(10 mmol) of 1 and 1.8 g(10.1 mmol) of *p*-chloromethyl benzoic acid were added into 25 ml flask containing 10 ml *o*-dichlorobenzene under N_2. After heating the mixture at 110 °C for 12 h, the precipitate was filtered and washed with acetone. 1.9 g of rose pink powder was obtained with no further purification, and the crude yield was 58%.

Sqb: 0.658 g (2 mmol) indolenine quaternary salt (2) and 0.114 g (1 mmol) squaric acid were heated in butanol (9 ml)/toluene (9 ml) mixture solvents with 5 ml pyridine as catalyst for 6 h [10]. The resulting precipitate was filtered and recrystallized from acetic acid to give 0.271 g of blue powder with 40% yield. Elemental analysis: calcd for $C_{42}H_{36}N_2O_6$ (%): C, 75.89; H, 5.46; N, 4.21; found, C, 75.81, H, 4.92, N, 3.95. ^{1}H NMR (400 MHz, DMSO): δ = 1.72(s, 12H, $C(CH_3)_2$), 5.48(s, 4H, N–CH_2), 5.77(s, 2H,=CH), 7.18(t, 2H, Ar–H), 7.26(m, 4H, Ar–H), 7.31(d, 4H, Ar–H, J = 8 Hz), 7.55(d, 2H, Ar–H, J = 7.6 Hz), 7.93(d, 4H, Ar–H, J = 8 Hz).

Cyb3: 0.658 g (2 mmol) of (2) was added into 25 ml flask containing 8 ml pyridine under N_2. After refluxing for 10 min, 0.9 ml (6 mmol) trimethyl orthoformate was added in portions. The resulting precipitate was recrystallized from acetone to give 0.750 g pink product with 60% yield. Elemental analysis: calcd for $C_{39}H_{37}ClN_2O_4$ (%): C, 73.98; H, 5.89; N, 4.42; found, C, 73.42, H, 5.23, N, 4.12. ^{1}H NMR (400 MHz, DMSO): δ = 1.73(s, 12H, $C(CH_3)_2$), 5.49(s, 4H, N–CH_2), 6.44(d, 2H, CH=CH, J = 13 Hz),7.29(m, 10H, Ar–H), 7.68(d, 2H, Ar–H, J = 7.6 Hz), 7.92(d, 4H, Ar–H, J = 8 Hz), 8.36(t, 1H, Ar–H, J = 13 Hz).

2.3. Preparation of nanoparticle colloid solution and nanocrystalline TiO_2 electrode

The preparation of TiO_2 nanoparticle colloid solution was prepared as described in ref [11]. A conductive glass of 2 cm × 2 cm cleaned with redistilled water was coated with TiO_2 nanoparticle colloid uniformly, and then heated to 450 °C for 30 min in the air, cooled down to room temperature (forming non-sensitized electrode) or to 80 °C, immediately soaked in methanol with concentration of 0.5 mmol L^{-1} dye for 12 h at room temperature, washed in ethanol, and finally dried in the air (forming sensitized electrode). The amount of adsorbed dye was determined by spectroscopic measurement of dye desorbed from the semiconductor surface in dilute methanol solution of KOH. Film thickness was confirmed using a DEKTAK step apparatus.

2.4. Photoelectrochemical experiments

Photoelectrochemical measurements were made with a thin layer solar cell comprising of a nanocrystalline TiO_2 working electrode and a thin platinum layer sputtered on conducting glass as counter electrode. The redox electrolyte solution consisted of a mixture of LiI (0.3 mol L^{-1}), I_2 (0.03 mol L^{-1}), and PC (1,2-propanediol carbonate) as the solvent. The area of the semiconductor electrodes was 0.27 cm × 0.27 cm. In photocurrent-photovoltage characteristics measurement, a 150 W xenon lamp served as a light source. A high-intensity grating monochromator (DWA10, Optical instrument Factory, Beijing, China) was introduced into the path of the excitation beam to produce incident monochromatic light. Electrochemistry workstation (CHI650A, Chenhua instrument Company, Shanghai) was used to measure the working curve of the photoelectrode and white light as incident light. Light intensity meter (Model 550-1) was used and photocurrent reaction spectrum was corrected to normalization for light source spectrum. A three-electrode cell composed of a platinum wire as working electrode, a platinum slice as counter electrode, and Ag/AgCl as reference electrode. The supporting electrolyte was $NaClO_4$ (0.1 mmol L^{-1}).

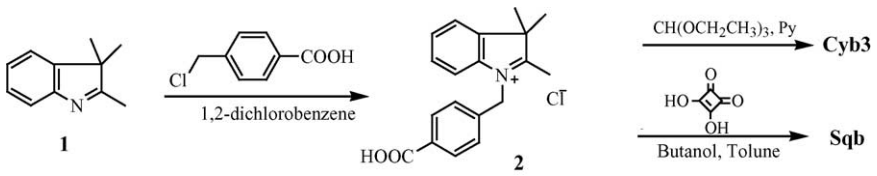

Scheme 1. Synthesis routes of Sqb and Cyb3.

2.5. Characterization of absorption spectra

JASCO V550 UV–vis and PTI-700 spectrophotometer were used to measure the absorption and emission spectra of the two dyes in methanol and sensitized electrode. References are methanol and indium stannum oxide conductive glass. All measurements were performed at room temperature.

3. Results and discussion

3.1. Synthesis and UV–vis spectral properties of Sqb and Cyb3 in solution

Cyb3 and Sqb with different methine chains have been synthesized (Scheme 1). The dyes can anchor on nano-TiO_2 surface via *N*-carboxylbenzyl group.

The absorption spectra of the two dyes in methanol are shown in Fig. 2. The spectral properties are summarized in Table 1. The λ_{max}^{abs} are 554 nm and 632 nm in methanol respectively, with a little negative solvatochromism from methanol to chloroform as solvent. The λ_{max}^{em} of Cyb3 is 573 nm with Stockes shift ($\Delta\lambda$) 19 nm in methanol. For Sqb, however, $\Delta\lambda$ is only 13 nm with λ_{max}^{em} 645 nm in methanol. Compared to Cyb3, λ_{max}^{abs} of Sqb shifts to the longer wavelength by ca. 80 nm with increasing length of the conjugated methine chain.

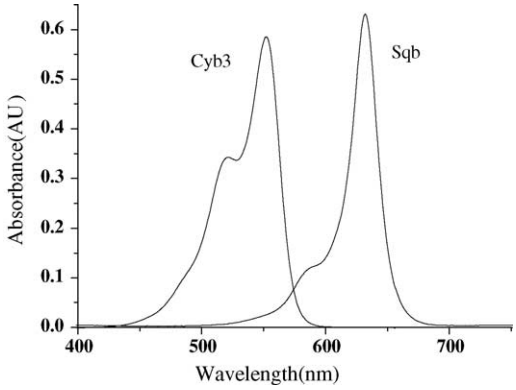

Fig. 2. Absorption spectra of Cyb3 and Sqb in methanol.

3.2. Energy level diagram

To judge the possibility of electron transfer from the excited dye molecules to the conductive band of TiO_2, cyclic voltammograms was performed to determine the redox potentials for the two dyes. Redox potentials of 0.37 V (versus SCE) or 0.61 V (versus NHE) or –5.45 eV (versus vacuum) and 0.32 V (versus SCE) or 0.58 V (versus NHS) or –5.42 eV (versus vacuum) averaging the related oxidation and reduction potentials are roughly regarded as the energy level of the ground state ($E^0(D^+/D)$) for Sqb and Cyb3 dye, respectively. Considering the UV–vis absorption spectra, the lowest energy of the excited state ($E^0(D^*/D^+)$) of the two dyes are about –3.62 eV (versus vacuum) and –3.26 eV (versus vacuum) (Eq. (1)). Major absorption at 550–680 nm and 450–570 nm wavelengths corresponds to the energy difference between the ground state and the lowest excited state (*E*g) of 1.83 eV and 2.16 eV for Sqb and Cyb3, respectively. Fig. 3 shows the energy level diagram of the two dyes in methanol. Obviously, the excited-state energy levels for the two dyes are more negative than the energy level of TiO_2 conductive band edge (–4.4 eV, versus vacuum) [1,12,13], suggesting that the electron injection should be possible thermodynamically. The driving force for charge displacement into the oxide is about 0.99 eV and 1.35 eV for Sqb and Cyb3, respectively. The redox potential of Sqb is less positive than the corresponding potential of Cyb3. The excited state of Sqb matches better with the lower bound of the conduction band of the semiconductor than the LUMO of Cyb3, thus decreas-

Table 1
Spectral properties of Cyb3 and Sqb in different solvents

Solvent	Cyb3			Sqb		
	λ_{max}^{abs} (nm)	λ_{max}^{em} (nm)	$\Delta\lambda$ (nm)	λ_{max}^{abs} (nm)	λ_{max}^{em} (nm)	$\Delta\lambda$ (nm)
Methanol	554	573	19	632	645	13
Ethanol	560	577	17	636	649	13
Acetonitrile	550	571	20	634	647	13
Chloroform	561	581	22	637	649	12

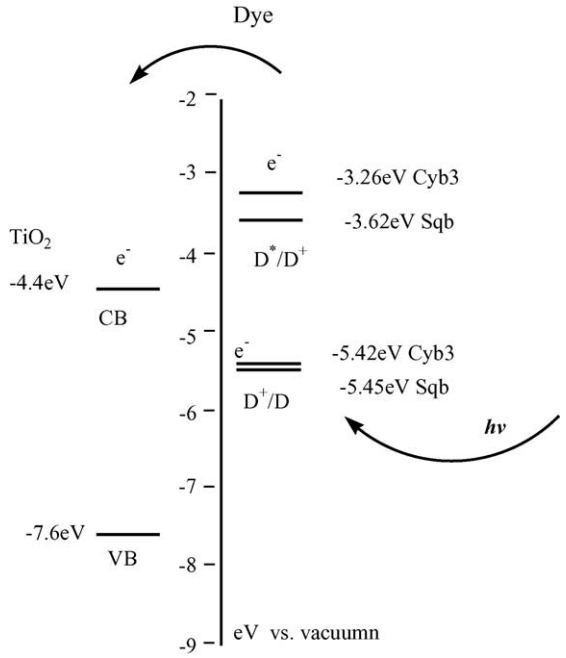

Fig. 3. Energy level diagram for Cyb3 and Sqb.

ing the energy loss during the electron transfer process.

$$E^0\left(\frac{D^*}{D^+}\right) = E^0\left(\frac{D^+}{D}\right) + Eg \quad (1)$$

3.3. Absorption spectra of the two dyes on TiO_2 electrode

The absorption peaks of the two dyes on TiO_2 films are all extremely broadened (Fig. 4) compared with their corresponding absorption peaks in methanol. It suggests that the dye molecules have formed H-aggregate or J-aggregate [14]. Fig. 5 is the proposed structure based on the geometry of the single crystal molecule (unpublished data). The dye moiety performs a plane due to the conjugated molecular structure and with the tilted large carboxylbenzyl group linked to the TiO_2 film surface via carboxylate form. To obtain the exact thickness of film and the optimal sensitized time, different sensitized conditions were investigated. 6.5 μm thickness of film and sensitized time of 4 h and 6 h for Cyb3 and Sqb are obtained, respectively.

3.4. Photoeletrochemical characteristics of solar cells

3.4.1. Photocurrent action spectra

Fig. 6 demonstrates the photocurrent action spectra of the dye-sensitized nanocrystalline TiO_2 electrodes normalized by incident light intensity for the two dyes. Sqb shows high light harvesting ability in the red visible region above 600 nm, which indicates that Sqb can expand the photoresponse of large band gap semiconductor TiO_2 into the red visible region. Comparing the action spectra with the absorption spectra of TiO_2 electrode sensitized by the dyes (Fig. 4),

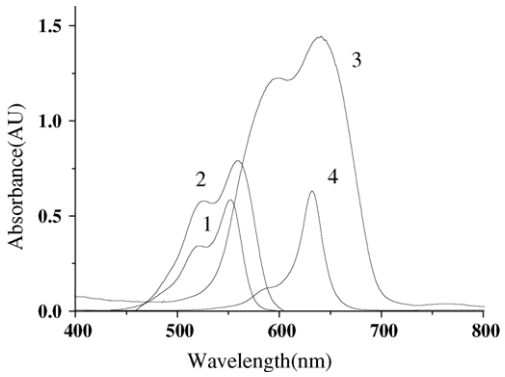

Fig. 4. (1) Absorption spectrum of Cyb3 in methanol, (2) absorption spectrum of TiO_2 electrode sensitized by Cyb3, (3) absorption spectrum of TiO_2 electrode sensitized by Sqb, and (4) absorption spectrum of Sqb in methanol. All electrodes were dried in air. Dyes were adsorbed in methanol solution (5×10^{-4} M). Total amount of the adsorbed dye was ca. 0.96×10^{-8} mol/cm^2 for Cyb3, 1.9×10^{-8} mol/cm^2 for Sqb, respectively.

the two dyes have spectra selectivity for different regions of visible light. Cyb3 converts more efficiently the light in the shorter wavelength region, but Sqb does in the long wavelength region. The action spectra and the absorption spectra of the two dyes resemble well, which indicates that the photocurrent is generated by the injection of electrons from the excited molecules into the conduction band of the TiO_2 electrode. Cyb3 and Sqb convert visible light to photocurrent in the region from 400 to 600 nm and 550 to 700 nm. The maximum IPCE values for Cyb3 and Sqb are about 36% and 46% respectively. The latter is 1.3 times much higher than that of the former. Therefore, Sqb has higher electron injection efficiency than Cyb3 dye.

IPCE is the monochromatic incident photon-to-current conversion efficiency, defined as the number of electrons injected by the excited dye in the external circuit decided by the number of incident photons, and is observed from the short-circuit photocurrents recorded at various excited wavelengths by means of the following expression:

$$\text{IPCE}\,(\%) = \frac{I}{P_{\text{in}}}\left(\frac{1240}{\lambda}\right) \quad (2)$$

where I is the short-circuit photocurrent (μA/cm^2), P_{in} is the incident light intensity (μW/cm^2) and λ is the excitation wavelength(nm).

3.4.2. Photocurrent-photovoltage characteristics curve and photoelectrochemical solar cells

The photocurrent and photovoltage curves are shown in Fig. 7. The photoelectrochemical properties of dye-sensitized TiO_2 electrode are given in Table 2.

Based on the characteristics curve, fill factor FF and the whole photo-electro transfer efficient η are obtained. FF is defined as

$$\text{FF} = \frac{P_{\max}}{V_{\text{oc}}\ I_{\text{sc}}} \quad (3)$$

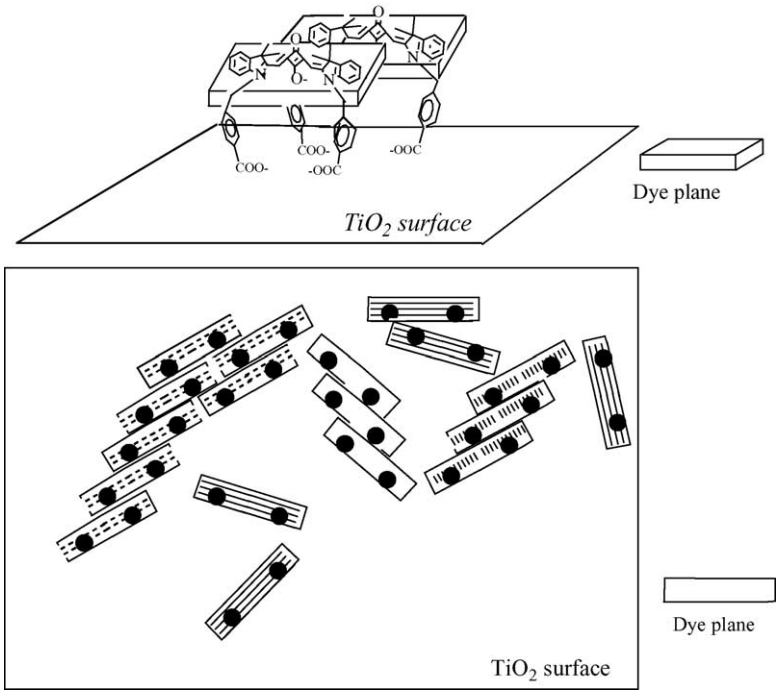

Fig. 5. (a) Proposed structure of the aggregated dyes on TiO_2 surface, (b) top view of the J-aggregated dyes on TiO_2 surface, closed circle is the carboxylbenzyl group anchoring on TiO_2 surface.

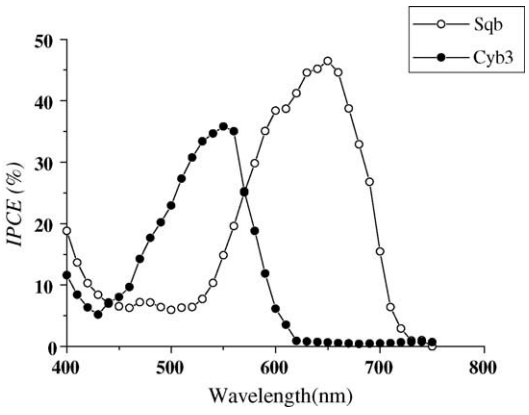

Fig. 6. Action spectra of the two dyes sensitized TiO_2 electrodes.

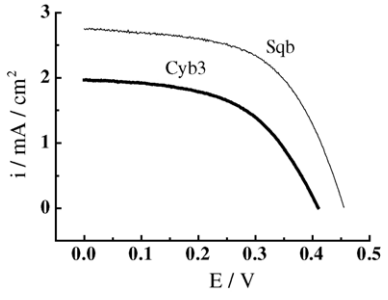

Fig. 7. Photocurrent and photovoltage curves.

Table 2
Parameters of the dye sensitized solar cells

	I_{sc}[a] (mA/cm^{-2})	V_{oc}[b] (mV)	FF[c]	η/%	T[d] (h)
Cyb3	1.97	410	0.527	1.01	4
Sqb	2.76	455	0.567	1.70	6

[a] I_{sc} is the short-circuit photocurrent.
[b] V_{oc} is the open-circuit voltage.
[c] FF is the fill factor of cell.
[d] T is the sensitized time, and film thickness is 6.5 μm, irradiated by 42 mW cm^{-2} white light.

where P_{max} is the largest output power of solar cells, I_{sc} is the short-circuit photocurrent, V_{oc} is the open-circuit photovoltage, η is defined as

$$\eta = \frac{\mathrm{FF}\ V_{oc}\ I_{sc}}{P_{in}} \quad (4)$$

where P_{in} is the input power.

From Table 2, the I_{sc} (2.76 mA/cm^2), IPCE (46%), and η (1.7%) of Sqb-sensitized TiO_2 solar cell performs preferable IPCE values to Cyb3 sensitized one.

Several reasons were considered to lead to the different photoelectric properties of the two TiO_2 electrodes sensitized by Sqb and Cyb3. Firstly, as a sensitizer for solar cells material, it must possess the high photostability. In Sqb dye structure, Squarylium ring substituted the conjugated chain, which leads to the dye more stable under irradiation [15]. And spectrum range of Sqb shifts to the long wavelength region, which is favorable to absorb solar light. Moreover, the lowest excited energy level of Sqb dye matches well to that of TiO_2 nanoparticle conductive band gap (Fig. 3). And the photoisomerization is one of the major decay pathways for methine dyes [16]. Sqb with methine chain substituted by squaric acid ring reduces cis-trans isomers. It is favorable to form ordered orientation on TiO_2 surface so as to increase the electron injection efficiency obviously.

4. Conclusions

In this article, we synthesized two novel cyanine dyes to be used as the sensitizer for solar cells material. The photoelectrochemical properties of TiO_2 nanocrystalline solar cells sensitized by the two dyes were investigated. The I_{sc} (2.76 mA/cm^2), IPCE (46%) and η (1.7%) of Sqb sensitized TiO_2 solar cell performs preferable IPCE values to that of Cyb3 sensitized one. The relationship of the molecule structure and the photoelectric properties were discussed which is important to design an efficient molecule sensitizer.

Acknowledgements

This work was financially supported by “973” programme of the ministry of Science and Technology of China and National Natural Science Foundation of China (20128005, 20376010).

References

[1] A. Hagfeldt, M. Grätzel, Chem. Rev. 95 (1995) 49.
[2] M.K. Nazeeruddin, A. Kay, K. Rodicio, T. Humphry-Baker, E. Muller, P. Liska, N. Vlachopoulos, M. Grätzel, J. Am. Chem. Soc. 115 (1993) 6382.
[3] O.B. Regan, M. Grätzel, Nature 353 (1991) 737.
[4] K. Hara, K. Sayama, Y. Ohga, A. Shinpo, S. Suga, H. Arakawa, Chem. Commun. 6 (2001) 569–570.
[5] T. Kitamura, M. Ikeda, K. Shigaki, T. Inoue, N.A. Anderson, X. Ai, T.Q. Lian, S. Yanagida, Chem. Mater 16 (2004) 1806–1812.
[6] K. Sayama, S. Tsukagoshi, K. Hara, Y. Ohga, A. Shinpou, Y. Abe, S. Suga, H. Arakawa, J. Phys. Chem. B. 106 (2002) 1363–1371.
[7] K. Sayama, S. Tsukagoshi, T. Mori, K. Hara, Y. Ohga, A. Shinpou, Y. Abe, S. Suga, H. Arakawa, Sol. Energy Mater. Sol. Cells 80 (2003) 47–71.
[8] X. Chen, Z.G. Yao, Chem. J. Chin. Univ. 17 (1996) 1613–1616.
[9] R.B. Mujumdar, L.A. Ernst, S.R. Mujumdar, C.J. Lewis, A.S. Waggoner, Bioconjug. Chem. 4 (1993) 105.
[10] H.E. Sprenger, W. Ziegenbeim, Angew. Chem. Int. Ed. 6 (1967) 553.
[11] Y.C. Shen, L. Wang, Z.H. Lu, Y. Wei, Chin. J. Mater. Res. 9 (1995) 81.
[12] P. Liska, N. Ulachopoulos, J. Am. Chem. Soc. 110 (1988) 3686.
[13] R. Vogel, P. Hoyer, H. Weller, J. Phys. Chem. 98 (1994) 3183.
[14] A. Mishra, R.K. Behera, P.K. Behera, B.K. Mishra, G.B. Behera, Chem. Rev. 100 (2000) 1973.
[15] W. Wang, Z.G. Yao, Photogr. Sci. Photochem. 15 (1997) 321–326.
[16] A.C. Khazraji, S. Hotchandani, S. Das, P.V. Kamat, J. Phys. Chem. B 103 (1999) 4693.